Neurobiology of Disease **8,** 667–678 (2001)
doi:10.1006/nbdi.2001.0398, *available online at http://www.idealibrary.com on* IDEAL®

β-Amyloid$_{(1-42)}$-Induced Cholinergic Lesions in Rat Nucleus Basalis Bidirectionally Modulate Serotonergic Innervation of the Basal Forebrain and Cerebral Cortex

Tibor Harkany,*,† Sheila O'Mahony,‡ Jan Keijser,* John P. Kelly,‡ Csaba Kónya,† Zsolt A. Borostyánkői,§,¶ Tamás J. Görcs,§ Márta Zarándi,‖ Botond Penke,‖ Brian E. Leonard,‡ and Paul G. M. Luiten*

**Department of Animal Physiology, University of Groningen, Kerklaan 30, NL-9750AA Haren, The Netherlands; †Trace-Element Research Center, Béres Co. Ltd., Budapest, Hungary; ‡Pharmacology Department, University College Galway, Galway, Republic of Ireland; §C&O Vogt Institute for Brain Research, University of Düsseldorf, Germany; ¶Neurobiological Research Group, United Research Organization of the Hungarian Academy of Sciences and Semmelweis University, Budapest, Hungary; and ‖Department of Medical Chemistry, University of Szeged, Szeged, Hungary*

Received July 3, 2000; revised December 12, 2000; accepted February 22, 2001

Ample experimental evidence suggests that β-amyloid (Aβ), when injected into the rat magnocellular nucleus basalis (MBN), impels excitotoxic injury of cholinergic projection neurons. Whereas learning and memory dysfunction is a hallmark of Aβ-induced cholinergic deficits, anxiety, or hypoactivity under novel conditions cannot be attributed to the loss of cholinergic MBN neurons. As mood-related behavioral parameters are primarily influenced by the central serotonergic system, in the present study we investigated whether Aβ$_{(1-42)}$ toxicity in the rat MBN leads to an altered serotonergic innervation pattern in the rat basal forebrain and cerebral cortex 7 days postsurgery. Aβ infusion into the MBN elicited significant anxiety in the elevated plus maze. Aβ toxicity on cholinergic MBN neurons, expressed as the loss of acetylcholinesterase-positive cortical projections, was accompanied by sprouting of serotonergic projection fibers in the MBN. In contrast, the loss of serotonin-positive fiber projections, decreased concentrations of both serotonin and 5-hydroxyindoleacetic acid, and decline of cortical 5-HT$_{1A}$ receptor binding sites indicated reduced serotonergic activity in the somatosensory cortex. In conclusion, the Aβ-induced primary cholinergic deficit in the MBN and subsequent cortical cholinergic denervation bidirectionally modulate serotonergic parameters in the rat basal forebrain and cerebral cortex. We assume that enhanced serotonin immunoreactivity in the damaged MBN indicates intrinsic processes facilitating neuronal recovery and cellular repair mechanisms, while diminished cortical serotonergic activity correlates with the loss of the subcortical cholinergic input, thereby maintaining the balance of neurotransmitter concentrations in the cerebral cortex. © 2001 Academic Press

Key Words: **β-Amyloid; anxiety; magnocellular nucleus basalis; serotonin; sprouting.**

Accumulation of β-amyloid peptides (Aβ) in the form of senile plaques in brain areas associated with learning and memory formation is one of the major neuropathological characteristics of Alzheimer's disease (AD; Iraizoz *et al.,* 1999; Selkoe, 1999; Sisodia & Price, 1995). Whereas a multitude of recent *in vitro* and *in vivo* investigations (Bruce-Keller *et al.,* 1998; Giovannelli *et al.,* 1995, 1998; Harkany *et al.,* 1995, 1999a,b; Laskay *et al.,* 1997; Mattson *et al.,* 1992; Yankner *et al.,* 1990) suggests potent neurotoxin-like properties for

0969-9961/01 $35.00

full-length Aβ, consisting of 42 amino acid residues ($A\beta_{(1-42)}$), specific molecular pathways by which Aβ compromise nerve cells still remain largely to be elucidated. Nevertheless, ample *in vitro* evidence points to an excitotoxin-like nature of Aβ (Cowburn *et al.*, 1994, 1997; Joseph & Han, 1992; Laskay *et al.*, 1997; Mattson *et al.*, 1992). *In vivo* experimental data in our laboratory substantiate Aβ excitotoxicity on cholinergic projection neurons of the rat magnocellular nucleus basalis (MBN), where Aβ toxicity was accompanied by an overt extracellular accumulation of excitatory amino acid neurotransmitters and by a pathologically increased intracellular Ca^{2+} accumulation (Harkany *et al.*, 1999a,b, 2000a). Taking previous findings together (Abe *et al.*, 1994; Giovannelli *et al.*, 1995, 1998; Harkany *et al.*, 1995, 2000a), it appears that cholinergic basal forebrain neurons are particularly vulnerable to Aβ toxicity.

Loss of cholinergic projection neurons in basal forebrain nuclei is a prominent neuropathological hallmark of AD (Bartus *et al.*, 1982; Mesulam, 1998; Whitehouse *et al.*, 1981), and closely correlates with the progressive loss of memory performance and with the degree of dementia (Iraizoz *et al.*, 1999). However, such a functional breakdown is not restricted to the cholinergic system, as the concurrent reduction of monoaminergic (e.g., serotonergic (5-HTergic) and noradrenergic (NEergic)) function was also associated with the pathogenesis of AD (Curcio & Kemper, 1984; Yamamoto & Hirano, 1985). Since 5-HTergic projection fibers originating in raphe nuclei are reported modulators of the function of cholinergic basal forebrain neurons (Khateb *et al.*, 1993; Smiley *et al.*, 1999), it seems likely that degeneration of postsynaptic cholinergic target cells may directly interact with the activity of the 5-HTergic projection system. Additionally, a cholinergic-5-HTergic interaction has also been established in the neocortex, where the two neurotransmitter systems share identical postsynaptic innervation targets, and coregulate a number of processes that are substantially involved in the regulation of learning and mood (Cassel & Jeltsch, 1995; Nilsson *et al.*, 1988; Riekkinen *et al.*, 1990). Accordingly, ample pharmacological evidence indicates that altered central 5-HTergic activity is critically involved in the development of fear, anxiety, and several mood-related psychiatric disorders (Chaouloff, 2000; File & Gonzalez, 1996; Leonard, 1996).

Previous *in vivo* studies demonstrated that infusion of Aβ fragments or the glutamate analogue *N*-methyl-d-aspartate (NMDA) into the rat MBN significantly affects locomotor activity (Harkany *et al.*, 1998), anxiety (Harkany *et al.*, 1999b, 2000b), and novelty-induced arousal (Harkany *et al.*, 2000b). Since changes of these behavioral parameters are presumably indirectly related to the primary cholinergic deficit following MBN lesions, in the present study we investigated whether $A\beta_{(1-42)}$ infusion into the MBN alters 5-HTergic responses in both the rat basal forebrain and cerebral cortex. Aβ was unilaterally injected into the MBN, and the degree of anxiety was assessed in the elevated plus maze test 7 days postsurgery. Aβ-induced damage to cholinergic MBN neurons was determined by means of quantitative acetylcholinesterase (AChE; EC 3.1.1.7) histochemistry in the somatosensory cortex, which receives the densest innervation from the damaged MBN subdivision (Luiten *et al.*, 1995). Alterations in the density of 5-HTergic fiber projections and of $5\text{-}HT_{1A}$ receptors were demonstrated both in the MBN and in the cerebral cortex. Additionally, Aβ-induced changes in serotonin (5-HT) and 5-hydroxyindoleacetic acid (5-HIAA) concentrations were measured in the somatosensory cortex.

MATERIALS AND METHODS

Peptide Synthesis

$A\beta_{(1-42)}$ was synthesized on an ABI 430 A automated peptide synthesizer (Biolytic Lab. Performance Inc., Fremont, CA) with amide at the C-terminal by a solid-phase technique involving Boc chemistry as previously described in detail (Harkany *et al.*, 1995, 2000a). Briefly, peptide chains were elongated on 4-methylbenzhydrylamine (MBHA) resin (0.6–0.8 mmol/g). Couplings were performed with dicyclohexylcarbodiimine with the exception of asparagine, which was incorporated in OHBt-ester form. The Boc group was removed by treatment with 50% trifluoroacetic acid in CH_2Cl_2. After completion of the synthesis, the peptides were cleaved from the resin with liquid hydrogen fluoride (HF). Free peptides were purified by reverse-phase high performance liquid chromatography (RP-HPLC) on an 8ST-SI-100S C_{18} column. Their purity was checked by RP-HPLC on a W-Porex $5C_{18}$ column. Amino acid analysis demonstrated the expected amino acid composition and electrospray mass spectrometry confirmed the expected molecular ion.

Animals, Surgical Procedure, and Tissue Processing

Young adult male Wistar rats (Charles River, SPF, 250–300 g, $n = 70$ [$n = 4$–7 per group]) were caged

individually at least 3 days prior to the start of the experiments and kept on a normal laboratory diet and tap water *ad libitum* in an air-conditioned room (21 ± 2°C) with a 12-h light / dark cycle (lights on at 08.00). All efforts were made to minimize animal suffering throughout the experiments. Their care and treatment were in accordance with the European Communities Council Directive (86 / 609 / EEC) and approved by the Local Ethical Committee of the University of Groningen (DEC #2286 / 1999).

The animals were anesthetized with halothane (1.5%, 1.8 L / min airflow; Zeneca, Ridderkerk, The Netherlands), and their heads were mounted in a stereotaxic frame (Narishige, Japan). Subsequently, for behavioral and quantitative histochemical studies, and for the determination of 5-HT_{1A} receptor density by means of autoradiography 1 μl of 200 μM $A\beta_{(1-42)}$ was injected slowly (0.1 μl / min) into the right MBN with a Hamilton microsyringe (anterior-posterior (AP) co-ordinate = −1.5 mm, L = 3.2 mm, DV = 6.5 mm; Paxinos & Watson, 1986), while for biochemical assays (5-HT and 5-HIAA) 2 μl of 200 μM $A\beta_{(1-42)}$ was delivered unilaterally. Previous studies in our laboratory demonstrated that infusion of 2 μl of $A\beta_{(1-42)}$ in the rat MBN produces characteristic biochemical changes in rat neocortex (Harkany *et al.*, 1995; O'Mahony *et al.*, 1998). Aliquots of lyophilized $A\beta_{(1-42)}$ were dissolved in ultrapure water and immediately infused into the MBN (O'Mahony *et al.*, 1998). All solutions were prepared freshly. Sham-operated animals received vehicle injections only. Based on previous evidence a 7-day survival period was used (Harkany *et al.*, 2000a; O'Mahony *et al.*, 1998).

For histochemistry, fixation of the brains was carried out under deep sodium pentobarbital anesthesia by transcardial perfusion with 350 ml fixative composed of 4% paraformaldehyde (PFA) in 0.1 M phosphate buffer (PB, pH 7.4), which was preceded by a short prerinse (50 ml) with physiological saline. Brains were then postfixed for 2 h in the same fixative, and cryoprotected by overnight storage in 30% sucrose in 0.1 M PB at 4°C. Thereafter, coronal frozen sections were cut on a cryostat microtome at 20- and 50-μm thickness for AChE histochemistry and 5-HT immunocytochemistry, respectively. For biochemical determination of cortical 5-HT and 5-HIAA concentrations and for the localization of 5-HT_{1A} receptors rats were deeply anaesthetized in ether and decapitated. Whole brains were quickly removed from the skull and stored at −80°C until further processing.

Elevated Plus Maze

To assess the effect of $A\beta_{(1-42)}$ infusion in the MBN on novel stimulation-evoked fear / anxiety as well as on exploratory drive the animals were tested in the elevated plus maze on day 7 (d7) postinjection according to a standard protocol (File & Gonzales, 1996; Harkany *et al.*, 1999b). Briefly, the plus maze had two open arms (50 × 10 cm) surrounded by 0.5-cm-high ledges and two closed arms of the same size with walls 50 cm high, elevated 50 cm above the ground. Each rat was placed in the central square of the apparatus (10 × 10 cm), facing a closed arm, and allowed to explore the maze for 5 min. The times spent on the open arms and the number of both open and closed arm entries were recorded. Additionally, the percentage time spent on the open arms and the percentage of open arm entries (time spent on open arms / total time × 100) [%t] and (open arm entries / total number of entries × 100) [%no]) were calculated. An increase in the percentage of the time spent on the open arms was interpreted as an anxiolytic response. All tests started at 11.00 a.m., and took place under quiet conditions in an environment lit by red light to force the animals to explore the plus maze apparatus.

Quantitative Histochemistry

For AChE histochemistry, free-floating sections were post-fixed by immersion in a 2.5% glutardialdehyde solution in phosphate-buffered saline (PBS; 0.01 M, pH 7.4) overnight at 4°C. Subsequently, cholinergic fibers were visualized by staining for AChE according to Hedreen *et al.* (1985) using an $AgNO_3$ intensification procedure.

Tissue sections processed for 5-HT immunocytochemistry were rinsed several times in 0.01 M PBS, immersed in 0.3% H_2O_2 in phosphate-buffered saline (0.01 M, pH 7.4; PBS) for 15 min, rinsed again, exposed to 0.5% Triton X-100 for 30 min, and incubated for 1 h at room temperature (RT) in 5% normal goat serum (NGS; Zymed, San Francisco, CA) diluted in 0.1% Triton X-100 and 0.1% sodium-azide-containing PBS. Subsequently, free-floating sections were incubated with rabbit anti-5-HT IgG, as primary antibody (diluted 1:10000; Freund *et al.*, 1990; Görcs *et al.*, 1985) in 1% NGS and 0.1% Triton X-100 at 4°C for 72 h under gentle movement of the incubation medium. After incubation, sections were thoroughly rinsed in PBS, preincubated for 1 h with 5% NGS at RT followed by the second antibody incubation with biotinylated goat anti-rabbit IgG (1:300; overnight at 4°C; Vector Labo-

ratories, Burlingame, CA) in PBS to which 1% NGS and 0.1% Triton X-100 had been added. Thereafter, sections were rinsed at least four times in PBS before the third incubation step (2 h at RT) using a conventional ABC detection protocol (Vectastain Elite ABC detection kit, 1:300; Vector Laboratories). Finally, tissue-bound peroxidase was visualized by means of 3,3′-diaminobenzidine (DAB) as chromogen (25 mg/100 ml) and 0.01% H_2O_2. Omission of the primary antibody yielded no detectable immunolabeling (data not shown).

AChE fiber density was measured in layer V of the posterior somatosensory cortex according to a standard protocol by using a Quantimet Q-600HR computerized image analysis system (Leica, Rijswijk, The Netherlands; Harkany *et al.*, 1999a, 2000b). Surface area density of cortical AChE-positive fibers was measured in three somatosensory cortical sections (at coordinates −1.3 mm, −1.5 mm, and −1.7 mm; Paxinos & Watson, 1986). After background subtraction and gray-scale threshold determination, the surface area of skeletonized AChE-positive fibers ([the area covered by AChE-positive cholinergic fibers]/[the total sampling area], given as percentages) was computed in each parietal cortical section by using a 599-nm emission filter. The relative value of fiber reduction was calculated in preestablished quadrants as the percentage difference between the surface area density at lesioned and contralateral sides of the brain.

The density of 5-HT immunoreactive (5-HT-ir) projections in the MBN and in the somatosensory cortex was determined by an unbiased, random sampling-based method utilizing computer-assisted (Quantimet Q-600HR, Leica) optical densitometry (Harkany *et al.*, 2000b). Briefly, at least three coronal sections were selected from each brain sample at identical AP coordinates (starting at −1.4 mm from bregma; Paxinos & Watson, 1986) with a standard distance of 100 μm. Following manual delineation, the extent of the intermediate MBN (mm^2) was determined. As inconsistent surface area determination may be a major pitfall of such a quantitative approach, special attention was given to the standardization of this particular step. Such data were therefore subjected to statistical analysis with nonsignificant differences between the different experimental groups as an obligate prerequisite of further data processing (contralateral hemisphere: 0.573 ± 0.026 mm^2 [sham-operated], 0.581 ± 0.027 mm^2 [A$\beta_{(1\text{-}42)}$] vs ipsilateral hemisphere: 0.596 ± 0.026 mm^2 [sham-operated], 0.581 ± 0.039 mm^2 [A$\beta_{(1\text{-}42)}$]). Thereafter, a frame grid consisting of 80 primary quantification frames of 110 × 110-μm individual frame size (as 8 frames/lane in 10 consecutive lanes) was superimposed. Each primary quantification frame was generated adjacent to the previous one (without any overlap) to ensure complete coverage of the region of our interest, but with the preservation of the independence of optical density (OD) measurements. Following subsequent threshold determination OD values were independently measured in all primary quantification frames that were in superposition with the delineated MBN structure. In general terms, such a quantification setup yielded 45–55 independent OD values covering the delineated MBN surface depending on the AP coordinates of the sections analyzed. OD values ranged from 0.000–2.500 based on standardized gray-scale values after logarithmic correction. Densitometrically obtained data were subsequently analyzed to determine (1) the mean ± SEM OD value of 5-HT-ir projections in each MBN, and (2) the distribution of OD values for the primary quantification frames at both sides of the brain.

Mean OD. Absolute OD values were averaged for each MBN and subsequently, the average of such values was calculated in the four sections analyzed. To express the effects of A$\beta_{(1\text{-}42)}$ infusion on 5-HT-ir structures these values were further processed to test statistically significant differences.

Distribution of independent OD values of primary quantification frames. Gray-scale-based OD determination employs distinct values between 0.000–2.500. Therefore, this range was divided into 25 identical subsets (e.g., 0.0–0.099, 0.1–0.199, etc.) and, accordingly, the frequency of independent measurements in the MBN was grouped and plotted. Such an approach reveals even mild shifts in ODs irrespective of their direction (increasing ODs: rightward, decreasing ODs: leftward) with high sensitivity.

5-HT-ir in cerebral cortex. 5-HT densitometry was only performed in layer V of the somatosensory cortex in sections adjacent to those stained for AChE. As 5-HTergic innervation of layer V of the cerebral cortex exhibits homogeneous staining intensities mean ± SEM OD values were expressed, whereas an OD distribution curve was not plotted.

5-HT_{1A} Receptor Autoradiography and Optical Densitometry

Localization of 5-HT_{1A} receptors in the MBN and somatosensory cortex was performed as essentially described by Nyakas *et al.* (1997) using [^{3}H]8-OH-DPAT (2(*N*,*N*-di[2,3(*n*)-^{3}H]propylamino)-8-hydroxytetralin, sp act: 221 Ci/mmol; Amersham Life Sci-

ences, Little Chalfont, Buckinghamshire, UK). Briefly, 20-μm-thick coronal brain sections were cut on a cryostat microtome and mounted onto electrically charged SuperFrost slides (Fisher Scientific, Tustin, CA). Subsequently, the sections were incubated in Tris–HCl buffer (0.17 M, pH 7.6) supplemented with 4 mM $CaCl_2$, 0.01% ascorbate and 10 μM pargyline for 60 min at RT. All chemicals were of analytical purity and purchased from Sigma (St. Louis, MO). Following incubation, the sections were washed 3 × 15 min at 4°C and air-dried. Nonspecific binding was determined in the presence of 1 μM 5-HT. Thereafter, sections were exposed to ^{3}H-sensitive Amersham Hyperfilm (Amersham) for 8 weeks at RT.

Autoradiograms were quantified by using an automated computer-assisted image analysis system (Q-500HC, Leica). After gray-scale threshold determination and background subtraction, OD of [^{3}H]8-OH-DPAT binding was determined as tissue equivalents (nCi/mg tissue) based on standard [^{3}H]Micro-scales (Amersham) and expressed as fmol/mg tissue. Specific binding was defined by subtracting tissue equivalent nonspecific binding separately in each cortical layer. In each brain, three sections were measured at AP coordinates corresponding to those selected for quantitative AChE histochemistry without preliminary knowledge of the case condition, and the average specific binding value of the three measurements was further processed statistically.

Determination of 5-HT and 5-HIAA Concentrations in the Neocortex

Biochemical analysis of 5-HT and 5-HIAA concentrations in the neocortex was carried out by means of HPLC with electrochemical detection as initially described by Seyfried *et al.* (1986). Briefly, neocortical samples were sonicated in 1 ml buffer (pH 2.8, adjusted with 4 N NaOH) containing 0.1 M citric acid, 0.1 M NaH_2PO_4, 1.4 mM octane-1-sulfonic acid, 0.1 mM etylenediaminetetraacetic acid, and 9% ethanol (mobile phase) to which 2 ng/50 μl *N*-methyl-dopamine had been added as internal standard that allowed correction for processing losses. Subsequently, aliquots were injected onto a LI Chrosorb RP-18 column and neurotransmitter fractions were detected electrochemically at 0.8V, with a mobile phase flow rate of 1 ml/min at a pressure of 200 bar. These data, together with those of the external standards were used to calculate 5-HT and 5-HIAA concentrations of the samples. Data were expressed as ng/g fresh weight of tissue.

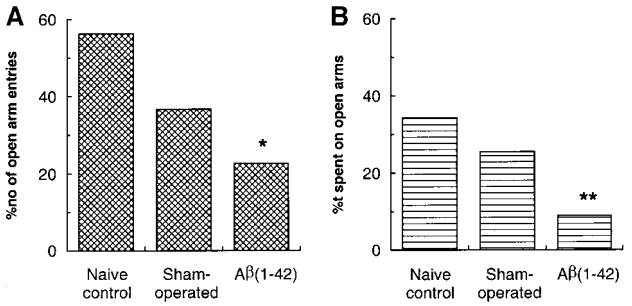

FIG. 1. Effect of $A\beta_{(1-42)}$ infusion in the MBN on elevated plus maze behavior of rats 7 days postsurgery. $A\beta_{(1-42)}$ elicited apparent anxiety in the plus maze as it was indicated by the significantly decreased percentages of open arm entries (%no, A) and the time spent on the open arms of the apparatus (%t, B), relative to both naive control and sham-operated animals. $^{**}P < 0.01$, $^{*}P < 0.05$, $A\beta_{(1-42)}$ [$n = 7$] vs naive controls [$n = 11$], or sham-operated animals [$n = 6$] (Mann–Whitney test). Data are presented as medians.

Statistical Analysis

Results on altered animal behavior were statistically evaluated with the nonparametric Mann–Whitney *U* test (Minitab, Release 9.2, 1993, Minitab Inc., State College, PA). Mann–Whitney *U* test was also applied for comparison of the effects of Aβ and vehicle infusions on 5-HT immunoreactivity in the MBN following transformation of OD values (Minitab, Release 9.2, 1993). Analysis of AChE-positive cortical innervation, the density of [^{3}H]8-OH-DPAT binding sites as well as 5-HT and 5-HIAA contents in the neocortex were calculated by one-way analysis of variance (ANOVA; SPSS for Windows, Release 9.0.1, SPSS Inc., Chicago, IL). A *P* level of < 0.05 was considered as indicative of statistical significance for the tests. Data on behavioral parameters were presented as medians, whereas changes in immunoreactivity or in biochemical parameters were expressed as means ± SEM.

RESULTS

$A\beta_{(1-42)}$ infusion in the MBN elicited anxiety in the elevated plus maze on *d7* postsurgery (Figs. 1A and 1B). Such a behavioral response was characterized by the significantly decreased frequency of open arm entries (22.69% (Aβ-lesioned) and by the apparently reduced time spent on the open arms of the apparatus (8.95% (Aβ-lesioned), as compared to both naive control and sham-lesioned animals (%no: 36.65% (sham-operated), 56.25% (naive control) (medians), $W = 11.96$, $P < 0.01$; Fig. 1A; %t: 25.50% (sham-operated), 34.33% (naive control), $W = 15.18$, $P < 0.01$; Fig. 1B).

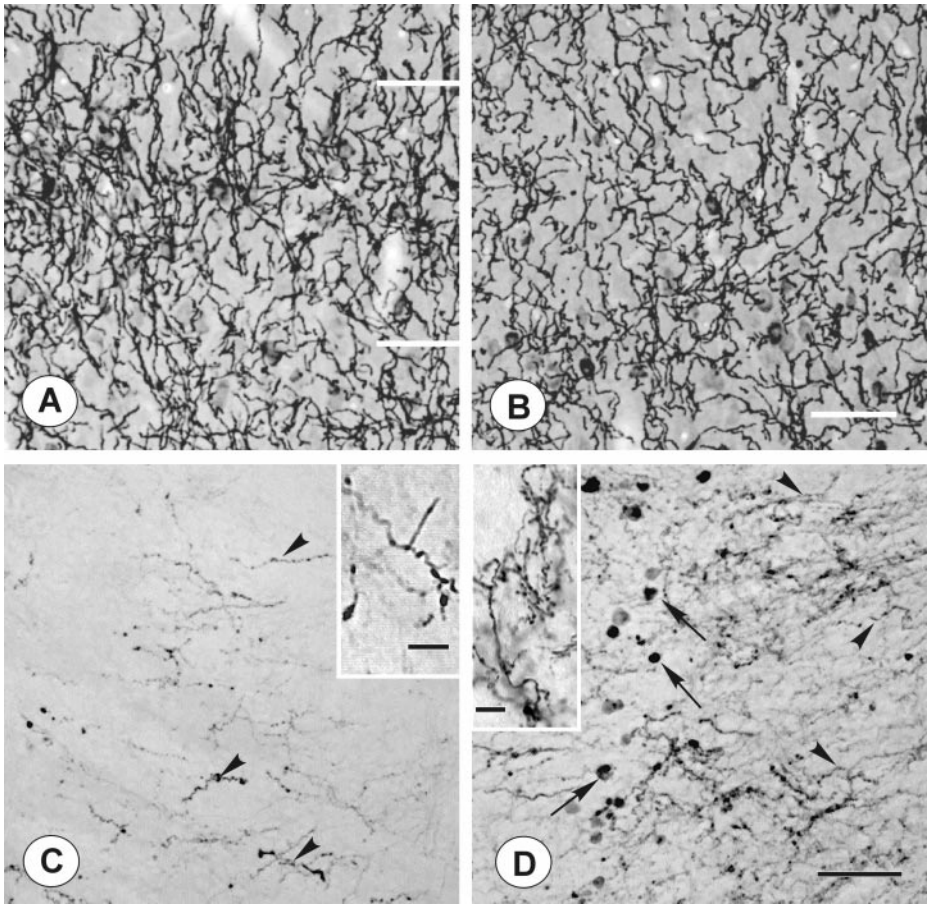

FIG. 2. Effect of A$\beta_{(1-42)}$ infusion on cortical cholinergic projections (A, B), and 5-HTergic innervation in the MBN (C, D). Note the apparent loss of acetylcholinesterase (AChE)-positive projection fibers in layer V of the somatosensory cortex (B), and the accumulation of 5-HT-ir projection neurites surrounding the A$\beta_{(1-42)}$-induced lesion (D), as compared to the effects of the sham-operative insult (A, C). Insets in Figs. C and D show representative 5-HT-immunoreactive projections in the MBN. Arrowheads point to sprouting 5-HTergic fibers, whereas arrows denote swollen—presumably degenerating—5-HT-positive varicosities in the core of A$\beta_{(1-42)}$ lesion. Horizontal bars in Fig. A denote the cortical layer, which was subjected to quantitative determination of surface area density of AChE-positive structural elements. Scale bar: (A) 50 μm; (D) 150 μm; (insets) 20 μm.

In accordance with previous data (Harkany *et al.*, 2000a; O'Mahony *et al.*, 1998), AChE histochemistry revealed a significant loss of cholinergic projection fibers invading the somatosensory cortex after A$\beta_{(1-42)}$ injections (Fig. 2B), relative to the sham-operated control group (Fig. 2A). Quantitative analysis of the density of AChE-positive projections in layer V of the somatosensory cortical area indicated 18.47 $\pm$ 1.62% reduction of cholinergic fiber processes as a consequence of A$\beta_{(1-42)}$ infusion that significantly exceeded the effects of sham-operation (6.85 $\pm$ 1.09%, $F = 11.72$, $P = 0.008$; Fig. 3A).

A$\beta_{(1-42)}$-induced lesions of the MBN elicited a bidirectional change in the density of 5-HTergic innervation of the rat forebrain. Neurotoxic lesions resulted in a strongly *increased* density of 5-HT fiber innervation in the lesioned cholinergic MBN (Fig. 2D), while in sham-lesioned animals only a lightly stained 5-HTergic projection network was present (Fig. 2C). Whereas the compact core of the A$\beta_{(1-42)}$ lesion was virtually devoid of 5-HT-ir fibers, two morphologically distinct types of 5-HTergic fibers were visualized in a strictly organized distribution pattern surrounding the A$\beta_{(1-42)}$-induced lesion. While 5-HT-positive fibers with swollen spherical or oval varicosities encircled the core of the lesion, a network of smooth 5-HT-ir fibers was predominantly present more distally in a likely "penumbra zone." As Fig. 3B shows, increased OD of the 5-HTergic innervation of the damaged MBN became apparent following analysis of

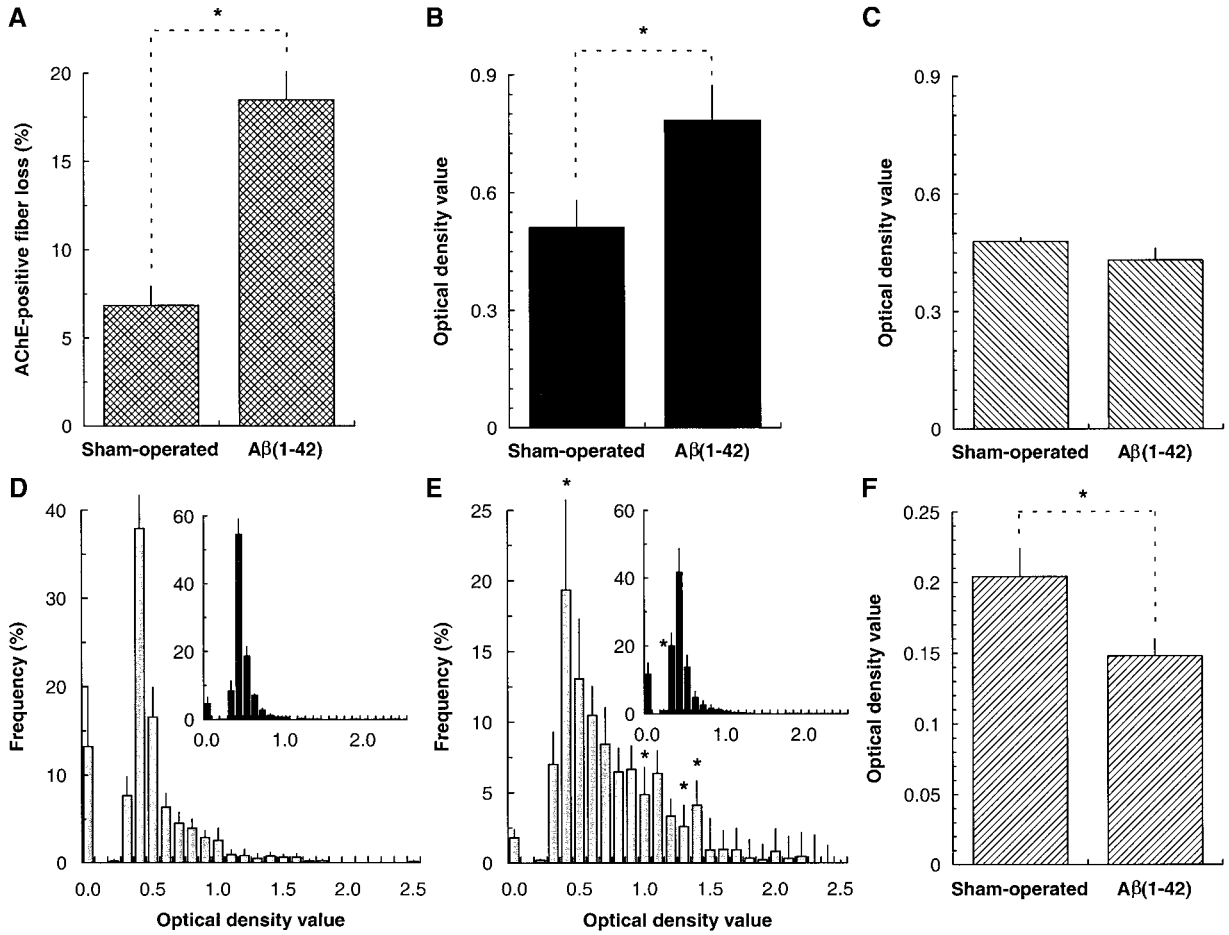

FIG. 3. Changes of cortical cholinergic innervation (A) and the density of 5-HTergic projections in the MBN (B–E) and in the neocortex (F) as a result of $A\beta_{(1\text{-}42)}$ infusion into the intermediate MBN subdivision, as detected by means of quantitative AChE histochemistry and 5-HT immunocytochemistry. $A\beta_{(1\text{-}42)}$ elicited a significant loss of cortical cholinergic innervation (A). Such a cholinotoxic injury was accompanied by sprouting of 5-HT-ir projection fibers in the ipsilateral MBN, as it was indicated by an increase in the mean optical density (OD; B) and by a considerable rightward shift in the OD distribution profile (E), and by decreased OD of cortical 5-HTergic projections (F), as compared to the effects of sham-operation (B, D). Note that unilateral Aβ infusion did not affect 5-HTergic activity in the contralateral MBN (mean OD, C; OD distribution, D, E insets), or in somatosensory cortex (data not shown). $^*P < 0.05$ vs sham-operated ($n = 6$).

mean OD values (0.78 ± 0.09 ($A\beta_{(1\text{-}42)}$-lesioned) vs 0.51 ± 0.07 (sham-operated), $F = 5.46$, $P < 0.05$). Distribution analysis of the OD values of primary quantification frames further substantiated the significant increase of 5-HT labeling in the ipsilateral MBN, as it was indicated by a shift towards higher individual gray-scale values of the primary quantification frames following $A\beta_{(1\text{-}42)}$ infusion, with significant differences at ODs ranging from 0.400–0.499, 1.000–1.099, 1.300–1.399, and 1.400–1.499 (Fig. 3E), as compared to sham-operated controls ($P < 0.05$; Fig. 3D). Analysis of the contralateral MBN following either $A\beta_{(1\text{-}42)}$ or sham lesions did not reveal significant differences either in the mean OD value (0.43 ± 0.03 ($A\beta_{(1\text{-}42)}$-lesioned) vs 0.48 ± 0.02 (sham-operated); Fig. 3C), or in the OD distribution profile of 5-HT-ir projection fibers (Figs. 3D and 3E, inset).

In contrast, a significantly *decreased* 5-HT signal was detected in layer V of the somatosensory cortex 7 days after $A\beta_{(1\text{-}42)}$ infusion in the MBN, as compared to the effects of sham operation (0.15 ± 0.01 ($A\beta_{(1\text{-}42)}$) vs 0.21 ± 0.02 (sham-operated), $F = 5.41$, $P < 0.05$; Fig. 3F), whereas 5-HT immunoreactivity in the contralateral neocortex was not altered (0.18 ± 0.03 ($A\beta_{(1\text{-}42)}$) vs 0.17 ± 0.04 (sham-operated).

Localization of 5-HT_{1A} receptors in the MBN by means of [^{3}H]8-OH-DPAT autoradiography revealed a slight, nonsignificant decrease in the density of

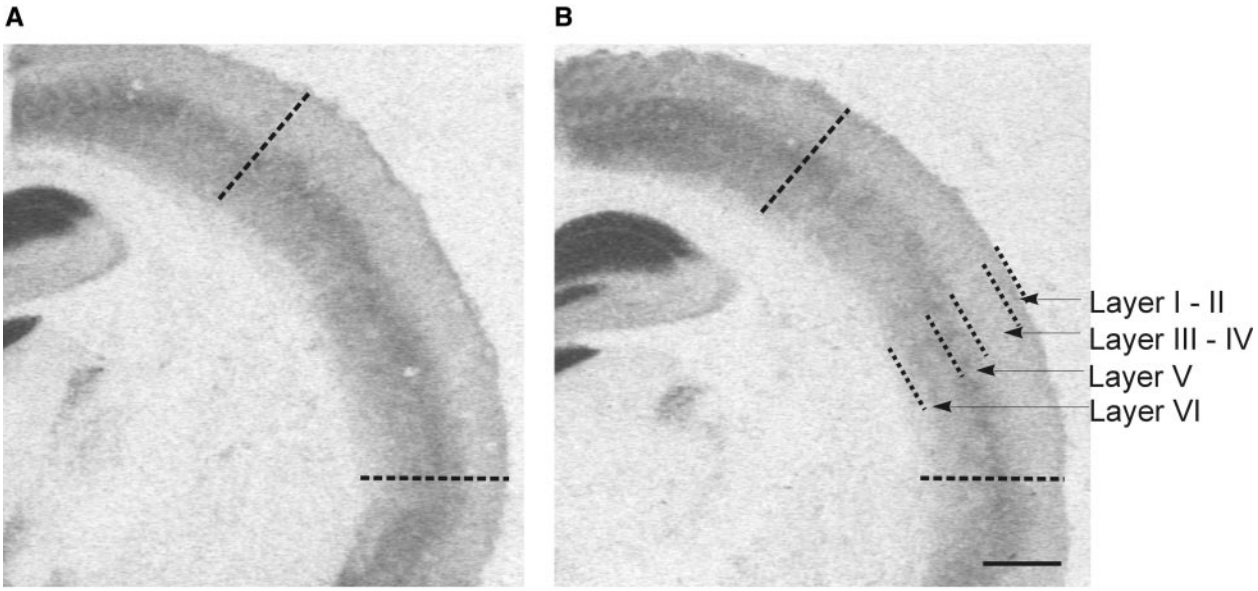

C

	Layer I - II	Layer III - IV	Layer V	Layer VI	*Entire Cortex*
Sham-operated (n = 4)	11.40 ± 0.91	11.72 ± 0.54	26.92 ± 1.22	17.61 ± 0.95	16.21 ± 0.36
Aβ(1-42) (n = 4)	9.41 ± 0.95	10.36 ± 1.13	22.31 ± 1.13*	13.48 ± 1.0.9*	13.85 ± 0.41*

FIG. 4. Distribution of [^{3}H]8-OH-DPAT binding in the parietal cortex after vehicle (A) or A$\beta_{(1-42)}$ (B) infusion into the MBN (−1.7 mm from bregma, Paxinos & Watson, 1986). Quantitative densitometric analysis was carried out in the cortical area bordered by dashed lines. Distinct neocortical layers were separated based on their different [^{3}H]8-OH-DPAT binding capacities, as shown in B. A significant decrease of [^{3}H]8-OH-DPAT binding was determined as a consequence of A$\beta_{(1-42)}$ infusion into the MBN (C). *$P < 0.05$ (one-way analysis of variance), data on [^{3}H]8-OH-DPAT binding were expressed as fmol/mg tissue based on standard [^{3}H]Micro-scales. Scale bar, 1 mm.

[^{3}H]8-OH-DPAT binding sites following A$\beta_{(1-42)}$ infusion (1.86 ± 0.30 fmol/mg tissue), as compared to the effect of sham-operation (2.15 ± 0.36 fmol/mg tissue). It is noteworthy, however, that the low density of 5-HT$_{1A}$ receptors on diffusely localized cholinergic neurons of the rat MBN is close to the sensitivity threshold of the detection procedure, as gray-scale values of the samples usually do not exceed that of the lowest standard point (1.4 nCi/mg tissue) of the [^{3}H]Microscales applied to plot a logarithmic calibration curve. As it is shown in Figs. 4A and 4B, the cortical binding pattern of [^{3}H]8-OH-DPAT closely resembled the distribution profile of AChE-positive cholinergic innervation fibers (Fig. 2B). Quantitative analysis of the distinct cortical layers, in particular of layer I-II, III-IV, V, and VI revealed a consistent decrement of [^{3}H]8-OH-DPAT binding in each neocortical layer investigated, with significant differences in layer V (17.14 ± 4.20% loss of the sham-operated value, $F = 7.10$, $P < 0.05$), layer VI (23.39 ± 6.16% loss of the sham-operated value, $F = 7.67$, $P < 0.05$), and in the [^{3}H]8-OH-DPAT binding of the entire neocortex (14.53 ± 2.51% of the sham value, $F = 16.58$, $P < 0.05$; Fig. 4C).

Concomitant with the loss of [^{3}H]8-OH-DPAT binding sites, significant reduction of 5-HT and 5-HIAA concentrations was measured in the somatosensory cortex as a consequence of A$\beta_{(1-42)}$ infusion in the MBN (Figs. 5A and 5B). A$\beta_{(1-42)}$ injections resulted in a 59.37 ± 4.43% decrease of the neocortical 5-HT concentration (314.1 ± 34.3 (A$\beta_{(1-42)}$) vs 773 ± 98.6 (sham-operated) ng/g tissue; $F = 4.41$, $P < 0.05$; Fig. 5A), which was paralleled by the levels of the 5-HT metabolite 5-HIAA. In fact, A$\beta_{(1-42)}$ induced a significant 55.34 ± 3.87% decline in cortical 5-HIAA concentration (199.3 ± 17.3 [A$\beta_{(1-42)}$] vs 446.3 ± 77.2 (sham-operated) and 415.6 ± 48.9 (naive control) ng/g tissue; $F = 3.44$, $P < 0.05$; Fig. 5B). It is noteworthy that sham-operation resulted in increased cortical 5-HT levels (543.5 ± 64.1 ng/g tissue), which were nonsig-

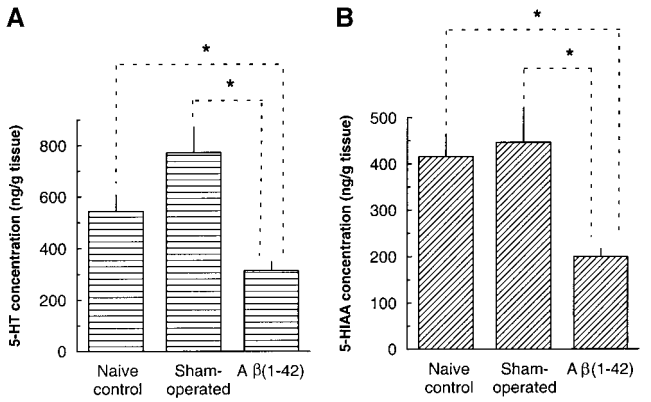

FIG. 5. Depletion of cortical serotonin (5-HT; A) and 5-hydroxyindoleacetic acid (5-HIAA; B) concentrations 7 days after $A\beta_{(1-42)}$ infusion in the rat MBN. Note the pronounced reduction of both 5-HT and 5-HIAA levels following $A\beta_{(1-42)}$ infusion. *Points to statistical significance ($P < 0.05$, analysis of variance). Data on at least six animals were used in each group for statistical analysis. 5-HT and 5-HIAA concentrations were expressed as ng/g tissue; data are presented as means ± SEM.

nificantly different from those of the naive control group.

DISCUSSION

The present data indicate that Aβ-induced injury to cholinergic neurons of the basal forebrain elicits anxiety-driven escape behavior in the elevated plus maze. A bi-directional change in 5-HTergic innervation of MBN and the cerebral cortex provided anatomical correlate for the Aβ-induced loss of cholinergic MBN neurons and their cortical projections 7 days post-lesion. Whereas abundant *accumulation* of 5-HT-ir fibers became evident in the close proximity of the neurotoxic lesion in the MBN, a significant *decrease* in the density of 5-HTergic projections paralleled the Aβ-induced decrement of cholinergic innervation in the cerebral cortex. Additionally, a significant loss of 5-HT_{1A} receptor-binding sites and concomitant reduction of 5-HT and 5-HIAA concentrations substantiated the decline of 5-HTergic input to the cerebral cortex.

Lesions to basal forebrain cholinergic nuclei were previously shown to impair sensory information processing in several learning paradigms (Harkany *et al.*, 1998, 1999a,b; Riekkinen *et al.*, 1990), whereas relatively little is known about their involvement in the development of anxiety (Harkany *et al.*, 2000b). As connection of monoaminergic, particularly 5-HTergic and NEergic systems to the development of anxiety is a well-established phenomenon (Chaouloff, 2000; Leonard, 1996; Ressler & Nemeroff, 2000), anxiety-related behavioral consequences of MBN lesions may implicate changes of the monoaminergic innervation of the basal forebrain and/or its projection areas, such as the somatosensory cortex. Hence, we investigated as to whether changes in escape behavior may be linked to altered 5-HTergic innervation of the MBN following $A\beta_{(1-42)}$ infusion.

Aβ infusion into the MBN results in the accumulation of 5-HT-ir projection fibers in a concentric fashion. Accordingly, 5-HT-ir fibers can be sub-divided into three major morphologically distinct categories: (a) the lesion core devoid of 5-HTergic sprouting, (b) inner zone with large (swollen) varicose 5-HT-positive fibers, and (c) a marginal "penumbra-like" zone of the neurotoxic lesion containing smooth 5-HTergic fibers. The "beaded" appearance of 5-HT-ir neurites in the inner zone of $A\beta_{(1-42)}$ lesions resembles morphological characteristics of degenerating 5-HTergic projection fibers during aging and in AD (Whitehouse *et al.*, 1981). We assume therefore that such 5-HTergic projections in the inner zone of Aβ lesion may undergo neurodegeneration as they lose their postsynaptic cholinergic targets or can directly be damaged by high concentrations of Aβ. Another explanation for the morphological diversity of 5-HT fibers may derive from the capacity of adult 5-HT fibers of heterotypic sprouting in response to damage of their postsynaptic targets, as it was shown after excitotoxic lesions to MBN, hippocampus, and striatum (Harkany *et al.*, 2000b; Zhou *et al.*, 1995). As the degree of 5-HTergic sprouting in the MBN closely correlates with the loss of AChE-positive projections in the somatosensory cortex ($5\text{-HT} = 0.426 + 0.0128\ \text{AChE}$, corr. coeff = 0.8486, $F = 30.88$, $P < 0.01$), we suggest that the density of 5-HTergic sprouting may correlate with the degree of neuronal damage elicited by Aβ.

It is well established that Aβ when injected into the basal forebrain initiates a glutamate-triggered excitotoxic cascade, which impels the degeneration of cholinergic projection neurons (Harkany *et al.*, 2000a). It should be noted that sprouting of monoaminergic projection fibers is not a unique Aβ-related phenomenon (Gasser & David, 1987; Peterson, 1994; Zhou *et al.*, 1995) and, particularly, can be triggered by a variety of excitotoxins, such as ibotenic acid (Zhou *et al.*, 1995) or NMDA (Harkany *et al.*, 2000b). Hence, it cannot be ruled out that changes in the density of 5-HTergic innervation appear as a consequence of altered local glutamate signaling and stimulation of glutamatergic receptors situated on 5-HTergic terminals, and are at

least partly unrelated to the loss of postsynaptic target neurons. From a functional point of view, if such a 5-HTergic sprouting response also leads to concomitant increase of 5-HT concentrations in the damaged MBN, as was shown in rat striatum after ibotenic acid injection (Zhou *et al.*, 1995), then it might be interpreted as a potential intrinsic defense mechanism in response to focal excitotoxic injury. Subsequently, 5-HT may act on 5-HT_{1A} receptors of cholinergic MBN neurons (Nyakas *et al.*, 1997) and thereby counteract excitotoxicity *via* antagonism of voltage-dependent Ca^{2+} channel currents (Bayliss *et al.*, 1997; Strosznajder *et al.*, 1996) and postsynaptic membrane hyperpolarization (Davies *et al.*, 1987; Williams *et al.*, 1998).

Another plausible explanation for 5-HTergic sprouting after $A\beta_{(1-42)}$ infusion may rise from the observation that $A\beta$ accumulation in plaques may induce aberrant axonal sprouting and formation of ectopic terminals in amyloid precursor protein (APP) transgenic mice (Phinney *et al.*, 1999). Accordingly, exogenous $A\beta_{(1-42)}$ infusion in the MBN might have initiated the 5-HTergic sprouting response in our present model. An additional factor triggering the observed axonal sprouting may be APP itself, as it is known that APP expression significantly and persistently increases following MBN lesions (Wallace *et al.*, 1991), APP may play a role in synapse formation and neurite extension (Allinquant *et al.*, 1995), and α-secretase-cleaved APP isoforms may be involved in neuroprotective mechanisms following acute brain damage (Mattson, 1997).

Depletion of 5-HTergic activity in the cerebral cortex has long been regarded as an early hallmark of neurodegenerative disorders (Palmer, 1996; Sparks, 1989). Neuropathological findings are supported by experimental data indicating the involvement of cortical 5-HTergic innervation in cognition in a substantial interaction with subcortical cholinergic efferents (Dringenberg & Zalan, 1999; Nilsson *et al.*, 1988; Riekkinen *et al.*, 1990). Our present data substantiate earlier observations on a close relationship between cortical cholinergic and 5-HTergic systems, as $A\beta$-induced damage to cholinergic MBN neurons and the concomitant loss of their cortical projections resulted in a marked decline of the density of 5-HT-ir projections, the number of 5-HT_{1A} receptors-binding sites and that of 5-HT and 5-HIAA concentrations in the somatosensory cortex. The simultaneous decrease of the 5-HTergic parameters investigated may hint compensatory down-regulation of cortical 5-HTergic activity in correlation with the decline of the subcortical cholinergic input instead of metabolic dys-balance (alteration in the 5-HT/5-HIAA ratio), or profound changes in postsynaptic 5-HT_{1A} receptor sensitivity. In functional terms, the simultaneous decline of cholinergic and 5-HTergic activity in the cerebral cortex may lead to decreased behavioral responsiveness under novel conditions and to increased anxiety/fear-related escape behavior. As development of anxiety correlates with the decrease of brain 5-HT function (Leonard, 1996), the plastic response of 5-HT innervation to $A\beta$-induced cholinergic hypo-activity in the rat neocortex provides neurochemical substrates to the apparent behavioral dysfunctions.

In conclusion, our present findings show that the loss of cholinergic projection neurons in the MBN as a consequence of $A\beta$-induced brain damage bidirectionally modulates 5-HTergic activity in the basal forebrain and cerebral cortex. The above-characterized interactions of basal forebrain cholinergic and raphe 5-HTergic systems may provide vistas for the development of neuroprotective drugs and therapeutic strategies that beneficially influence AD-related loss of memory functions.

ACKNOWLEDGMENTS

The authors acknowledge the expert assistance of S. J. Elzinga and J. Mulder during initial phase of the behavioral and histochemical experiments, and Dr. E. A. Van der Zee for his helpful comments on the design of the quantification protocol for 5-HT. This work was supported by the *Hungarian National Science Foundation* (OTKA, F023865 to T.H., T022546 to M.Z., and T017751 to B.P.).

REFERENCES

Abe, E., Casamenti, F., Giovannelli, L., Scali, C., & Pepeu, G. (1994) Administration of amyloid β-peptides into the medial septum of rats decreases acetylcholine release from hippocampus *in vivo*. *Brain Res.* **636,** 162–164.

Allinquant, B., Hantraye, P., Mailleux, P., Moya, K., Bouillot, C., & Prochiantz, A. (1995) Downregulation of amyloid precursor protein inhibits neurite outgrowth *in vitro*. *J. Cell Biol.* **128,** 919–927.

Bartus, R. T., Dean, R. L. 3rd, Beer, B., & Lippa, A. S. (1982) The cholinergic hypothesis of geriatric memory dysfunction. *Science* **217,** 408–414.

Bayliss, D. A., Li, Y.-W., & Talley, E. M. (1997) Effects of serotonin on caudal raphe neurons: Inhibition of N- and P/Q-type calcium channels and the afterhyperpolarization. *J. Neurophysiol.* **77,** 1362–1374.

Bruce-Keller, A. J., Li, Y.-J., Lovell, M. A., Kraemer, P. J., Gray, D. S., Brown, R. R., Markesbery, W. R., & Mattson, M. P. (1998) 4-Hydroxynonenal, a product of lipid peroxidation, damages cholinergic neurons and impairs visuospatial memory in rats. *J. Neuropathol. Exp. Neurol.* **57,** 257–267.

Cassel, J.-C., & Jeltsch, H. (1995) Serotonergic modulation of cholinergic function in the central nervous system: Cognitive implications. *Neuroscience* **69,** 1–41.

Chaouloff, F. (2000) Serotonin, stress and corticoids. *J. Psychopharmacol.* **14,** 139–151.

Cowburn, R. F., Messamore, E., Li-Li, M., Winblad, B., & Sundström, E. (1994) β-Amyloid related peptides exert differential effects on [^{3}H]MK-801 binding to rat cortical membranes. *NeuroReport* **5,** 405–408.

Cowburn, R. F., Wiehager, B., Trief, E., Li-Li, M., & Sundström, E. (1997) Effects of β-amyloid-(25-35) peptides on radioligand binding to excitatory amino acid receptors and voltage-dependent calcium channels: Evidence for a selective affinity for the glutamate and glycine recognition sites of the NMDA receptor. *Neurochem. Res.* **22,** 1437–1442.

Curcio, C. A., & Kemper, T. (1984) Nucleus raphe dorsalis in the dementia of the Alzheimer-type: Neurofibrillary changes and neuronal packing density. *J. Neuropathol. Exp. Neurol.* **43,** 359–368.

Davies, M. F., Deisz, R. A., Prince, D. A., & Peroutka, S. J. (1987) Two distinct effects of 5-hydroxytryptamine on single cortical neurons. *Brain Res.* **423,** 347–352.

Dringenberg, H. C., & Zalan, R. M. (1999) Serotonin-dependent maintenance of spatial performance and electroencephalography activation after cholinergic blockade: Effects of serotonergic receptor antagonists. *Brain Res.* **837,** 242–253.

File, S. E., & Gonzalez, L. E. (1996) Anxiolytic effects in the plus-maze of 5-HT$_{1A}$-receptor ligands in dorsal raphe and ventral hippocampus. *Pharmacol. Biochem. Behav.* **54,** 123–128.

Freund, T. F., Gulyás, A. I., Acsády, L., Görcs, T., & Tóth, K. (1990) Serotonergic control of the hippocampus via local inhibitory interneurons. *Proc. Natl. Acad. Sci. USA* **87,** 8501–8505.

Gasser, U. E., & Dravid, A. R. (1987) Noradrenergic, serotonergic, and cholinergic sprouting in the hippocampus that follows partial or complete transection of the septohippocampal pathway: Contributions of spared inputs. *Exp. Neurol.* **96,** 352–364.

Giovannelli, L., Casamenti, F., Scali, C., Bartolini, L., & Pepeu, G. (1995) Differential effects of amyloid peptides β-(1-42) and β-(25-35) injections into the rat nucleus basalis. *Neuroscience* **66,** 781–792.

Giovannelli, L., Scali, C., Faussone-Pellegrini, M. S., Pepeu, G., & Casamenti, F. (1998) Long-term changes in the aggregation state and toxic effects of β-amyloid injected into the rat brain. *Neuroscience* **87,** 349–357.

Görcs, T. J., Liposits, Z., Chan-Palay, V., & Palay, S. L. (1985) Brain Surface Serotonergic Neurons. *Proc. Natl. Acad. Sci. USA* **82,** 7449–7452.

Harkany, T., Ábrahám, I., Laskay, G., Timmerman, W., Jost, K., Zarándi, M., Penke, B., Nyakas, C., & Luiten, P. G. M. (1999a) Propionyl-IIGL tetrapeptide antagonizes β-amyloid excitotoxicity in rat nucleus basalis. *NeuroReport* **10,** 1693–1698.

Harkany, T., Ábrahám, I., Timmerman, W., Laskay, G., Tóth, B., Sasvári, M., Kónya, C., Sebens, J. B., Korf, J., Nyakas, C., Zarándi, M., Soós, K., Penke, B., & Luiten, P. G. M. (2000a) β-Amyloid neurotoxicity is mediated by a glutamate-triggered excitotoxic cascade in rat nucleus basalis. *Eur. J. Neurosci.* **12,** 2735–2745.

Harkany, T., Dijkstra, I. M., Oosterink, B. J., Horvath, K. M., Ábrahám, I., Keijser, J., Van der Zee, E. A., & Luiten, P. G. M. (2000b) Increased amyloid precursor protein expression and serotonergic sprouting following excitotoxic lesions to the rat magnocellular nucleus basalis: Prevention by Ca^{2+} antagonist nimodipine. *Neuroscience* **101,** 101–114.

Harkany, T., Lengyel, Z., Soós, K., Penke, B., Luiten, P. G. M., & Gulya, K. (1995) Cholinotoxic effects of β-amyloid$_{(1-42)}$ peptide on cortical projections of the rat nucleus basalis magnocellularis. *Brain Res.* **695,** 71–75.

Harkany, T., Mulder, J., Sasvári, M., Ábrahám, I., Kónya, C., Zarándi, M., Penke, B., Luiten, P. G. M., & Nyakas, C. (1999b) *N*-methyl-d-aspartate receptor antagonist MK-801 and radical scavengers protect cholinergic nucleus basalis neurons against β-amyloid neurotoxicity. *Neurobiol. Dis.* **6,** 109–121.

Harkany, T., O'Mahony, S., Kelly, J. P., Soós, K., Törô, I., Penke, B., Luiten, P. G. M., Nyakas, C., Gulya, K., & Leonard, B. E. (1998) β-Amyloid(Phe(SO$_3$H)^{24})25-35 in rat nucleus basalis induces behavioral dysfunctions, impairs learning and memory and disrupts cortical cholinergic innervation. *Behav. Brain Res.* **90,** 133–145.

Hedreen, J. C., Bacon, S. J., & Price, D. L. (1985) A modified histochemical technique to visualize acetylcholinesterase-containing axons. *J. Histochem. Cytochem.* **33,** 133–140.

Iraizoz, I., Guijarro, L. J., Gonzalo, L. M., & de Lacalle, S. (1999) Neuropathological changes in the nucleus basalis correlate with clinical measures of dementia. *Acta Neuropathol.* **98,** 186–196.

Joseph, R., & Han, E. (1992) Amyloid protein fragment 25-35 causes activation of cytoplasmic calcium in neurons. *Biochem. Biophys. Res. Commun.* **184,** 1441–1447.

Khateb, A., Fort, P., Alonso, A., Jones, B. E., & Mühlethaler, M. (1993) Pharmacological and immunocytochemical evidence for serotonergic modulation of cholinergic nucleus basalis neurons. *Eur. J. Neurosci.* **5,** 541–547.

Laskay, G., Zarándi, M., Varga, J. L., Jost, K., Fonagy, A., Torday, C., Latzkovits, L., & Penke, B. (1997) A putative tetrapeptide antagonist prevents β-amyloid-induced long-term elevation of $[Ca^{2+}]_i$ in rat astrocytes. *Biochem. Biophys. Res. Commun.* **235,** 479–481.

Leonard, B. E. (1996) Serotonin receptors and their function in sleep, anxiety disorders and depression. *Psychother. Psychosom.* **65,** 66–75.

Luiten, P. G. M., Douma, B. R. K., Van der Zee, E. A., & Nyakas, C. (1995) Neuroprotection against NMDA induced cell death in rat nuclus basalis by Ca^{2+} antagonist nimodipine, influence of aging and developmental drug treatment. *Neurodegeneration* **4,** 307–314.

Mattson, M. P. (1997) Cellular actions of β-amyloid precursor protein and its soluble and fibrillogenic derivatives. *Physiol. Rev.* **77,** 1081–1132.

Mattson, M. P., Cheng, B., Davis, D., Bryant, K., Lieberburg, I., & Rydel, R. R. (1992) β-Amyloid peptides destabilize calcium homeostasis and render human cortical neurons vulnerable to excitotoxicity. *J. Neurosci.* **12,** 376–389.

Mesulam, M.-M. (1998) Some cholinergic themes related to Alzheimer's disease: Synaptology of the nucleus basalis, location of m2 receptors, interactions with amyloid metabolism, and perturbations of cortical plasticity. *J. Physiol. (Paris)* **92,** 293–298.

Nilsson, O. G., Strecker, R. E., Daszuta, A., & Björklund, A. (1988) Combined cholinergic and serotonergic denervation of the forebrain produces severe deficits in a spatial learning task in the rat. *Brain Res.* **453,** 235–246.

Nyakas, C., Oosterink, B. J., Keijser, J., Felszeghy, K., de Jong, G. I., Korf, J., & Luiten, P. G. M. (1997) Selective decline of 5-HT$_{1A}$ receptor binding sites in rat cortex, hippocampus and cholinergic basal forebrain nuclei during aging. *Chem. Neuroanat.* **13,** 53–61.

O'Mahony, S., Harkany, T., Rensink, A. A. M., Ábrahám, I., De Jong, G. I., Varga, J. L., Zarándi, M., Penke, B., Nyakas, C., Luiten, P. G. M., & Leonard, B. E. (1998) β-Amyloid-induced cholinergic denervation correlates with enhanced nitric oxide synthase activity in rat cerebral cortex: Reversal by NMDA receptor blockade. *Brain. Res. Bull.* **45,** 405–411.

Palmer, A. M. (1996) Neurochemical studies of Alzheimer's disease. *Neurodegeneration* **5,** 381–391.

Paxinos, G., & Watson, C. (1986) *The Rat Brain in Stereotaxic Coordinates.* 2nd ed. Academic Press, Sydney.

Peterson, G. M. (1994) Sprouting of central noradrenergic fibers in the dentate gyrus combined lesions of its entorhinal and septal afferents. *Hippocampus* **4,** 635–648.

Phinney, A. L., Deller, T., Stalder, M., Calhoun, M. E., Frotscher, M., Sommer, B., Staufenbiel, M., & Jucker, M. (1999) Cerebral amyloid induces aberrant axonal sprouting and ectopic terminal formation in amyloid precursor protein transgenic mice. *J. Neurosci.* **19,** 8552–8559.

Ressler, K. J., & Nemeroff, C. B. (2000) Role of serotonergic and noradrenergic systems in the pathophysiology of depression and anxiety disorders. *Depress. Anxiety* **12,** 2–19.

Riekkinen, P. Jr., Sirviö, J., & Riekkinen, P. (1990) Interaction between raphe dorsalis and nucleus basalis magnocellularis in spatial learning. *Brain Res.* **527,** 342–345.

Selkoe, D. J. (1999) Translating cell biology into therapeutic advances in Alzheimer's disease. *Nature* **399,** A23–A31.

Seyfried, C. A., Adam, G., & Greve, T. (1986) An automated direct-injection HPLC-method for the electrochemical/fluorimetric quantitation of monoamines and related compounds optimized for the screening of large numbers of animals. *Biomed. Chromatogr.* **1,** 78–88.

Sisodia, S. S., & Price, D. L. (1995) Role of the β-amyloid protein in Alzheimer's disease. *FASEB J.* **9,** 366–370.

Smiley, J. F., Subramanian, M., & Mesulam, M.-M. (1999) Monoaminergic-cholinergic interactions in the primate basal forebrain. *Neuroscience* **93,** 817–829.

Sparks, D. L. (1989) Aging and Alzheimer's disease. Altered cortical serotonergic binding. *Arch. Neurol.* **46,** 138–140.

Strosznajder, J., Chalimoniuk, M., & Samochocki, M. (1996) Activation of serotonergic 5-HT_{1A} receptors reduces Ca^{2+}- and glutamatergic receptor-evoked arachidonic acid and NO/cGMP release in adult hippocampus. *Neurochem. Int.* **28,** 439–444.

Wallace, W. C., Bragin, V., Robakis, N. K., Sambamurti, K., Vander-Putten, D., Merril, C. R., Davis, K. L., Santucci, A. C., & Haroutunian, V. (1991) Increased biosynthesis of Alzheimer amyloid precursor protein in the cerebral cortex of rats with lesions of the nucleus basalis of Meynert. *Mol. Brain Res.* **10,** 173–178.

Whitehouse, P. J., Price, D. L., Clark, A. W., Coyle, J. T., & DeLong, M. R. (1981) Alzheimer's disease: Evidence for selective loss of cholinergic neurons in the nucleus basalis. *Ann. Neurol.* **10,** 122–126.

Williams, S., Serafin, M., Mühlethaler, M., & Bernheim, L. (1998) The serotonin inhibition of high-voltage-activated calcium currents is relieved by action potential-like depolarizations in dissociated cholinergic nucleus basalis neurons of the guinea-pig. *Eur. J. Neurosci.* **10,** 3291–3294.

Yamamoto, T., & Hirano, A. (1985) Nucleus raphe dorsalis in Alzheimer's disease: Neurofibrillary tangles and loss of large neurones. *Ann. Neurol.* **17,** 573–577.

Yankner, B. A., Duffy, L. K., & Kirschner, D. A. (1990) Neurotrophic and neurotoxic effects of amyloid β protein: Reversal by tachykinin neuropeptides. *Science* **250,** 279–282.

Zhou, F. C., Azmitia, E. C., & Bledsoe, S. (1995) Rapid serotonergic fiber sprouting in response to ibotenic acid lesion in the striatum and hippocampus. *Dev. Brain Res.* **84,** 89–98.